The Journal of Experimental Biology 215, 3539-3551

doi:10.1242/jeb.070466

RESEARCH ARTICLE

On the ascent: the soleus operating length is conserved to the ascending limb of the force–length curve across gait mechanics in humans

Jonas Rubenson[1,*], Neville J. Pires[1], Heok O. Loi[1], Gavin J. Pinniger[2] and Damian G. Shannon[1]

[1]School of Sport Science, Exercise and Health, The University of Western Australia, Crawley, WA, 6009, Australia and
[2]School of Anatomy, Physiology and Human Biology, The University of Western Australia, Crawley, WA, 6009, Australia

*Author for correspondence (Jonas.Rubenson@uwa.edu.au)

SUMMARY

The region over which skeletal muscles operate on their force–length (F–L) relationship is fundamental to the mechanics, control and economy of movement. Yet surprisingly little experimental data exist on normalized length operating ranges of muscle during human gait, or how they are modulated when mechanical demands (such as force output) change. Here we explored the soleus muscle (SOL) operating lengths experimentally in a group of healthy young adults by combining subject-specific F–L relationships with *in vivo* muscle imaging during gait. We tested whether modulation of operating lengths occurred between walking and running, two gaits that require different levels of force production and different muscle–tendon mechanics, and examined the relationship between optimal fascicle lengths (L_0) and normalized operating lengths during these gaits. We found that the mean active muscle lengths reside predominantly on the ascending limbs of the F–L relationship in both gaits (walk, 0.70–0.94 L_0; run, 0.65–0.99 L_0). Furthermore, the mean normalized muscle length at the time of the peak activation of the muscle was the same between the two gaits (0.88 L_0). The active operating lengths were conserved, despite a fundamentally different fascicle strain pattern between walking (stretch–shorten cycle) and running (near continuous shortening). Taken together, these findings indicate that the SOL operating length is highly conserved, despite gait-dependent differences in muscle–tendon dynamics, and appear to be preferentially selected for stable force production compared with optimal force output (although length-dependent force capacity is high when maximal forces are expected to occur). Individuals with shorter L_0 undergo smaller absolute muscle excursions ($P<0.05$) so that the normalized length changes during walking and running remain independent of L_0. The correlation between L_0 and absolute length change was not explained on the basis of muscle moment arms or joint excursion, suggesting that regulation of muscle strain may occur *via* tendon stretch.

Key words: force–length, soleus, gait, muscle length, locomotion.

Received 19 January 2012; Accepted 18 June 2012

INTRODUCTION

One of the most important functional characteristics of skeletal muscle is the length dependence of its force-generating potential (force–length relationship). The force–length (F–L) relationship has typically been described from maximal isometric contractions, where the capacity to generate force is greatest at an optimal length (L_0), and falls with both increasing and decreasing muscle lengths relative to L_0 [descending and ascending limbs of the F–L curve, respectively (Hill, 1953; Gordon et al., 1966)].

The range over which a muscle operates on its F–L relationship critically influences locomotor performance (Rome, 1998; Rassier et al., 1999; Burkholder and Lieber, 2001). Muscle function at the plateau region of the F–L relationship may be regarded as favourable since maximal force output is achieved for a given level of muscle activation, thus providing optimal joint moment and/or mechanical work and power output. This strategy of optimizing force output has been directly observed in some animal studies, for example red muscle fibres in swimming carp (Rome and Sosnicki, 1991) and the frog semimembranosus muscle during jumping (Lutz and Rome, 1994).

In contrast to this view, it has been hypothesized that muscles function on the part of the F–L curve that matches the *in vivo* functional demand of the muscle (Herzog et al., 1992; Rassier et al., 1999). For example, a muscle that undergoes lengthening–shortening cycles generally increases force as it lengthens and decreases force as it shortens. Thus, operating on the ascending limb of the F–L curve would allow the length-dependent force-generating capacity of the muscle and the actual *in vivo* force required during the movement task (e.g. muscle force produced during stance in walking) to increase and decrease in parallel. Conversely, if the muscle were to lengthen on the descending limb of its F–L curve it will have a mismatch between its length-dependent force-generating capacity and the *in vivo* force requirement. Furthermore, it has been proposed that muscles are inherently more stable if they operate along the ascending limb of the F–L relationship, where any length perturbation experienced at the level of the muscle fibre creates an opposing force that will tend to restore the muscle length to a stable position (Julian and Morgan, 1979; Morgan, 1990). Muscles functioning on the descending limb of the F–L curve may be less suited to withstand lengthening perturbations linked to muscle injury and eccentric muscle damage, possibly as a result of non-uniform sarcomere lengthening (Hill, 1953; Morgan, 1990). Where muscles operate on their F–L curve and how their length operating ranges are modulated when different mechanical demands are placed on the muscle is important for understanding in more detail the control, mechanics and energetics of locomotion.

Although the region of the F–L curve occupied by muscles during locomotion has been primarily measured in non-human animals (Burkholder and Lieber, 2001), a handful of estimates have been made for leg muscles in human gait using both anatomical and computational approaches (Cutts, 1989; Fukunaga et al., 2002; Arnold and Delp, 2011). These studies have begun to shape our understanding of human muscle operating lengths during various locomotor tasks. Yet they each share a common limitation, namely the use of indirect (typically cadaveric) information on optimal muscle lengths, which in turn defines the region of the F–L curve occupied by the muscle. This limitation is important, especially considering that L_0 may vary between individuals, since muscle architecture is known to be different between cadavers and age-matched live individuals (Martin et al., 2001) and is affected by age and disuse (Narici and Maganaris, 2007). Furthermore, while computer-modelling approaches have several important merits, there exist uncertainties regarding how variables such as tendon stiffness and activation levels affect predictions of fibre lengths (Arnold and Delp, 2011). Given its fundamental significance to the mechanics of human movement, it is surprising that more direct experimental measurements of normalized length operating ranges of muscle during gait are lacking.

The primary objective of this study was to establish the region of the F–L curve occupied by the soleus muscle (SOL) during walking and running in young adults using a novel experimental framework. This study is, to the best of our knowledge, the first to relate experimental subject-specific muscle length changes during gait with an experimental subject-specific muscle F–L relationship, and thus represents a more direct analysis of the operating range of muscles across their F–L curve in human gait. We addressed three questions: (1) what is the total and active muscle length operating range of the SOL during gait; (2) is the SOL operating range modulated between walking and running, two basic modes of movement that are predicted to elicit different mechanical functions of the triceps surae muscles (Sasaki and Neptune, 2006; Lichtwark et al., 2007); and (3) how is the SOL operating range correlated with L_0? Notwithstanding its anatomical complexity (Hodgson et al., 2006), the SOL has been chosen because: (a) it is known to be among the most important muscles in the production of the forward propulsion of the centre of mass during walking and running (McGowan et al., 2009; Hamner et al., 2010), (b) because it permits an estimate of force and length in a single muscle of the triceps surae group [owing to the possibility to mitigate the force in the gastrocnemius muscles at flexed knee postures (Hof and van den Berg, 1977; Maganaris, 2001)] and (c) because it is a fatigue-resistant muscle (Kawakami et al., 2000), and thus more suitable to experimental protocols requiring repeated contractions.

MATERIALS AND METHODS

Subjects

Eight healthy, recreationally fit male subjects were recruited for this study (26±3.51 years of age and 70.31±9.18 kg; mean ± s.d.). The subjects were free of any musculoskeletal disorders or injuries at the time of testing. Subjects provided written, informed consent prior to partaking in the study. All of the procedures were approved by the Human Research Ethics Committee at The University of Western Australia.

Subject-specific passive and active force–length experiment

A dynamometer (M3, Biodex, Shirley, NY, USA) was used to determine the net passive and active moments developed across the participant's right ankle. Subjects were seated in the dynamometer using a custom-built rig that allowed their tibia to be positioned horizontally in a padded brace and their knee to remain at 130 deg flexion (Fig. 1A), and which minimized heel movement across the ankle range of motion. A flexed knee angle was adopted to mitigate the ankle moment contribution from the gastrocnemius muscles (Hof and van den Berg, 1977; Maganaris, 2001). This was confirmed in our participants as their maximal voluntary isometric plantar flexion torque did not change between knee angles of 130–110 deg with a maximally dorsiflexed ankle. A sensitivity analysis further indicated that the gastrocnemius and other synergist muscles influence the F–L relationship minimally (see Appendix).

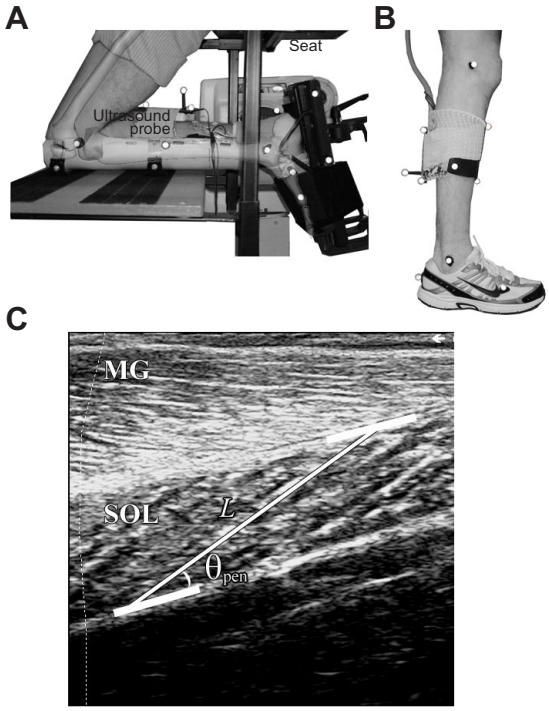

Fig. 1. The experimental set-up for measuring subject-specific F–L properties of the human soleus muscle (SOL). (A) Dynamometer joint positioning and ultrasound placement during the F–L experiment. (B) Position of the ultrasound probe for muscle scanning and segment and ultrasound markers used for walking and running trials. (C) Representative ultrasound image of the SOL fascicles (the superimposed white lines represent the SOL aponeuroses and fascicle orientations). MG, medial gastrocnemius; θ_{pen}, pennation angle; L, fascicle length.

Prior to passive moment measurements, the subject's ankle was cycled through its range of motion three times. The ankle was randomly set to one of seven angles that spanned equally the joint range of motion, measured using a goniometer attached on the foot rig and off-line from sagittal plane 2D video [Sony, DER-HE52E; 50 Hz; digitized using ImageJ software; NIH, Bethesda, MD, USA (Abramoff et al., 2004)]. The ankle angle was defined as per the International Society of Biomechanics standard ankle joint definition (Wu et al., 2002) (positive angles dorsiflexion, negative angles plantar flexion).

Measurements of passive moments were recorded at least 45 s after the ankle had been set to the desired angle to minimize elastic dissipative effects of the muscle–tendon unit. Each passive isometric trial was repeated a minimum of three times at each of the seven angles across the joint range of motion. To determine the contribution of the SOL fascicles to the net passive joint moment

($\mathbf{M}_{SOLp}$), the moments generated due to the weight of the footplate attachment ($\mathbf{M}_{rig}$) and the foot itself ($\mathbf{M}_{foot}$) were subtracted from the total Biodex moment ($\mathbf{M}_{tot}$). This was performed using a rig-only moment–angle measurement and an estimate of the weight of the foot (expressed as a percentage of body mass) and centre of mass (Winter, 1990).

Simultaneous measurements of fascicle lengths and pennation angles [ImageJ software (Abramoff et al., 2004)] were performed *in vivo* using B-mode ultrasound (EchoBlaster128, Telemed, Vilnius, Lithuania) with a low-profile (flat-shaped) multi-frequency linear array probe (60 mm field of view, 7 MHz scan frequency; 25 Hz capture rate) (Fig. 1B,C). To standardize the probe location across subjects, a location was defined over the medial gastrocnemius (MG) where the distal end of the probe was placed at the MG muscle–tendon junction. This location gave reliable ultrasound images of the SOL fascicles and aponeuroses and was reproducible across all subjects. The average of five frames was used for each trial. The ultrasound image was synchronized to analog data [joint moment and electromyography (EMG)] and video data *via* a 5 V TTL pulse.

Surface EMG (Motion Lab Systems, Baton Rouge, LN, USA) was recorded from the SOL, the MG and lateral gastrocnemius (LG) muscles and the tibialis anterior muscle (TA) using custom-made double-differential pre-amplifiers and electrodes (20–1000 Hz bandpass; 2000 Hz sample frequency). Only those trials with no EMG activity were included in further analyses of passive force. All analog signals were recorded using a CED data acquisition system running Spike2 V7 software (Micro1401-3; Cambridge Electronic Design, Cambridge, UK; 2000 Hz).

In each trial, the passive force in the Achilles tendon ($\mathbf{F}_{TENDp}$) was computed by dividing $\mathbf{M}_{SOLp}$ by a subject-specific Achilles tendon moment arm [SOL moment arm ($\mathbf{r}_{SOL}$)]. Achilles tendon moment arms were measured for each subject using the tendon travel method (An et al., 1984) from dynamic ultrasound scans of the MG muscle–tendon junction displacement and simultaneous ankle angle measurements. Because tendon stretch and tendon slack can invalidate the tendon travel method at high dorsiflexion (Maganaris, 2004) and plantar flexion angles (Herbert et al., 2011), respectively, we estimated the moment arms at the end ranges of motion using a scaled, subject-specific geometric model. This was achieved by modifying the muscle path in a subject-specific scaled OpenSim model (Arnold et al., 2010) so that the Achilles moment arm matched the experimental moment arm between –10 and 10 deg ankle angle (Fig. 2). The predicted moment arm from the model at maximum dorsiflexion was assessed by locating the Achilles tendon line of action relative to the ankle centre using ultrasound and video-imaging following the study of Manal et al. (Manal et al., 2010).

Passive fascicle force was calculated by dividing $\mathbf{F}_{TENDp}$ by the cosine of the measured SOL pennation angle ($\cos\theta_{pen}$). Finally, a passive fascicle F–L relationship was created by fitting the F–L data using an exponential equation (Gollapudi and Lin, 2009):

$$\mathbf{F}_{SOLp} = Ae^{b(L-L_S)}, \quad (1)$$

where L is the fascicle length and L_s is the length at which passive forces first appear; A and b are constants determined using non-linear least-squares fitting (lsqcurvefit function using MATLAB, MathWorks, Natick, MA, USA). Although other muscles and joint structures may contribute to some of the passive force, errors in the subsequent predictions of L_0 arising from these have been assessed to be small (see Appendix).

Initial baseline maximal voluntary isometric plantar flexion and dorsiflexion contractions (MVC) were performed at three angles spanning the ankle range of motion. The initial plantar flexion trials were used to provide reference maximal EMG values for the F–L experiment. The dorsiflexion trials were used for establishing maximal dorsiflexion joint moments and EMG values used for co-contraction calculations (see below). A minimum of three additional isometric plantar flexion MVCs were subsequently performed at each of seven randomized ankle angles over the same ankle angle range as the passive isometric trials. A rest period of 2 min was used between consecutive contractions to mitigate any effect of muscle fatigue on force output (Kawakami et al., 2000). For each MVC trial, a real-time root mean square (r.m.s.) wave of the SOL activity was computed from the EMG signals (incorporating DC offset; Spike2 V7 software) and expressed as a fraction of the initial peak baseline MVC r.m.s. This was done to ensure that subsequent MVCs remained at a near constant activation level. Only trials in which MVC r.m.s. values were within ±10% of the baseline MVCs were used for analysis. In order to further assess whether the participants were capable of achieving maximal contractions we subsequently performed twitch interpolation measurements during MVCs. Similar to previous findings on young men (Behm et al., 1996), maximal or near-maximal (>95%) activation was achieved at ankle angles across the joint range of motion, indicating that our estimate of L_0 was not affected by the inhibition of voluntary muscle activation (see

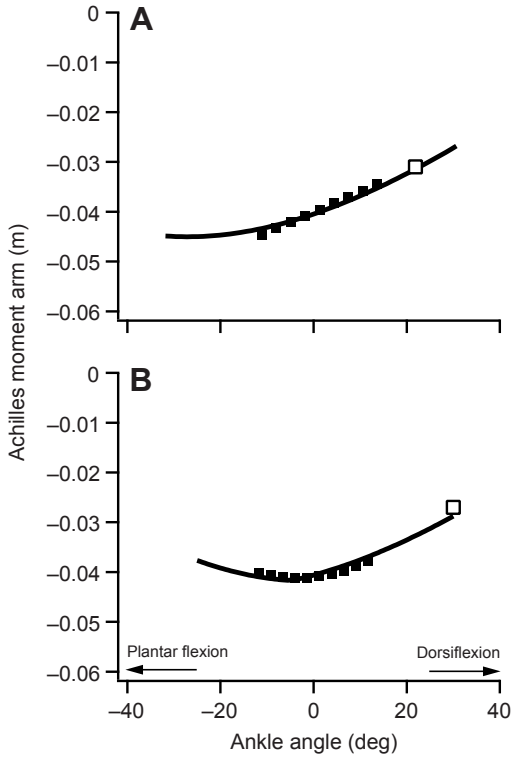

Fig. 2. Example experimental data (squares) and matched subject-specific modeled data (continuous line) for the Achilles moment arm from two representative subjects. Filled squares are data from ultrasound-based tendon travel experiments (Maganaris, 2004) and the open square represents the moment arm measured as the perpendicular distance from the line of action of the tendon to the joint centre using a combination of ultrasound imaging and video data (Manal et al., 2010). Achilles moment arms from tendon travel experiments were computed by differentiating either a second-order (A) or third-order (B) polynomial fitted to the tendon travel (m) *vs* joint angle (rad) data. A third-order polynomial was used only if the third term was statistically different from zero (P<0.05).

Appendix for detailed methods and limitations to MVC dynamometry assessments of peak force). An online r.m.s. MVC ratio was also implemented for the TA to estimate the level of co-contraction. A minimum of three MVC trials for each angle were used for establishing the active SOL F–L relationship.

The peak net ankle joint moment during the plantar flexion MVC ($\mathbf{M}_{peak}$) was calculated as the difference between the peak recorded Biodex moment during the MVC and the mean resting Biodex moment prior to the contraction. To take into account the effect of a reduction in passive fascicle forces during contraction due to fascicle shortening and tendon stretch prior to the isometric phase of the contraction (Zajac, 1989; MacIntosh and MacNaughton, 2005), passive forces in the fascicle were predicted for both the fascicle length at the MVC (peak moment) and the fascicle length during the rest period just prior to contraction using Eqn 1. The difference in the plantar flexor moment due to a reduction in passive force at the MVC compared with the rest length was calculated as:

$$\Delta\mathbf{M}_{SOLp} = \left(\mathbf{F}_{SOLp}^{peak} \times \cos\theta_{PEN}^{peak} \times \mathbf{r}_{SOL}^{peak}\right) - \left(\mathbf{F}_{SOLp}^{rest} \times \cos\theta_{PEN}^{rest} \times \mathbf{r}_{SOL}^{rest}\right), \quad (2)$$

where rest and peak superscripts designate rest or MVC, respectively. To account for the effect of co-contraction, the dorsiflexion moment developed by the TA ($\mathbf{M}_{TA}$) was computed using an estimate of its per cent activation from EMG and its dorsiflexion moment at maximal activation. Further details on this method and its effect on the F–L curve and estimated L_0 are detailed in the Appendix. Accounting for passive fascicle force and co-contraction, the active plantar flexion moment produced by the SOL was estimated: $\mathbf{M}_{SOLa}=(\mathbf{M}_{peak}-\Delta\mathbf{M}_{SOLp}-\mathbf{M}_{TA})$. Finally, the active SOL fascicle force was determined from the angle-specific SOL moment arm and fascicle pennation angle:

$$\mathbf{F}_{SOLa} = \frac{\mathbf{M}_{SOLa}}{\mathbf{r}_{SOL}^{peak} \times \cos\theta_{PEN}^{peak}} . \quad (3)$$

All calculations for passive and active F–L data were computed using a custom-written program in MATLAB.

Determination of optimal fascicle length (L_0)

The experimental L_0 was determined using a non-linear least-squares optimization routine implemented in MATLAB (*fmincon* function) that minimized the sum of the squared differences between the experimental normalized peak active fascicle forces and those calculated from a theoretical whole muscle F–L curve at the same normalized lengths. The theoretical curve was fitted with a cubic spline interpolation using the spline control points from the whole muscle active F–L curve provided in OpenSim (Delp et al., 2007). To ensure maximal force values were used, only the 10 peak values from the repeated trials across 10 equally spaced muscle length groupings were used. For the solution to be accepted, the L_0 solved for had to reside within the plateau region of the experimental F–L data, with increases in length resulting in constant or decreasing force. This approach not only assesses the muscle length at which peak force is achieved, but importantly, also incorporates the overall shape of the force–length curve in determining L_0.

Force–length operating range during walking and running

The F–L operating range of the right SOL during walking and running on a force-plate instrumented treadmill (Bertec, Columbus, OH, USA) was examined by integrating motion analysis, ultrasound, EMG and the subject's previously established F–L relationship within 2–3 days after the F–L assessments. The ultrasound probe location and orientation between experiments was maintained and assessed using a probe marker set and spatial measurements (for further details see Appendix). We examined two different speeds: (1) the subjects' preferred treadmill walking speed (assessed by varying speed by increments of $0.1\,m\,s^{-1}$), and (2) running at $3.0\,m\,s^{-1}$. Preferred speeds were chosen rather than a set speed given that they are known to be related to minimal energy expenditure (Ralston, 1958; Rubenson et al., 2007) and optimal muscle–tendon function (Neptune et al., 2008).

To determine the portion of the F–L curve that the SOL occupied during the walking and running trials, SOL fascicle lengths were imaged dynamically using B-mode ultrasound (70 Hz capture rate; data synchronization *via* TTL pulse). The ultrasound probe was secured to the participant's calf using an elastic bandage (Elastoplast Sport, Beiersdorf Australia, North Ryde, Australia; Fig. 1B). Muscle lengths were digitized in ImageJ, filtered using a fourth-order zero-lag 5 Hz low-pass Butterworth filter (MATLAB), and divided by L_0 in order to describe the portion of the F–L curve occupied by the muscle. Regions of the F–L curve occupied by the muscle were defined based on a whole muscle F–L curve: $L/L_0<0.75$, steep ascending limb; $0.75\leq L/L_0<0.95$, shallow ascending limb; $0.95\leq L/L_0\leq 1.05$, plateau region; $1.05<L/L_0$, descending limb (Arnold and Delp, 2011). These regions differ slightly from the theoretical sarcomere F–L curve and reflect sarcomere length heterogeneity in whole muscle.

Normalized muscle length data were compared with ankle joint angles and the SOL EMG during the gait trials. Ankle joint angles were computed from a 10-camera 3D motion capture system (Vicon, Oxford Metrics, Oxford, UK; 250 Hz) and a lower limb model developed within the UWA School of Sport Science, Exercise and Health (Besier et al., 2003). 3D trajectories of the lower limb markers were compiled and joint kinematics were modelled in Vicon Bodybuilder following the kinematic modelling techniques outlined in Besier et al. (Besier et al., 2003). The EMG signal was high-pass filtered, full-wave rectified and low-pass filtered using a fourth-order zero-lag Butterworth filter at 7 Hz to create an EMG liner envelope (MATLAB).

Statistics

SOL muscle length changes, EMG linear envelope and ankle joint angle from five strides per speed per subject were computed. Gait and muscle data were normalized to 101 points over one stride using a cubic spline interpolation to facilitate compilation of mean data from multiple trials for each individual. Mean individual data were compiled to calculate group mean data ± s.d. The muscle length characteristics were compared between walking and running trials using a paired sample, two-tailed Student's *t*-test at a significance level of $P<0.05$. Data are reported as group means ± s.d. unless otherwise stated.

RESULTS

Passive force–length relationship

The fascicle length where passive forces first appear (L_s) was 0.0377±0.0053 m. The mean L_s coincided closely with, and was not statistically different from, the mean optimal fascicle lengths (L_0; see below) calculated from the active F–L relationship (2.70±3.2 mm difference; $P=0.973$; $L_s/L_0=1.01\pm0.12$). The pooled normalized passive F–L data from the eight participants when fitted using Eqn 1 resulted in the estimated model parameters $A=2.380\times10^{-2}\pm2.80\times10^{-3}$ and $b=5.31\pm0.31$; $r^2=0.600$). The peak passive fascicle force was 887.9±282.8 N.

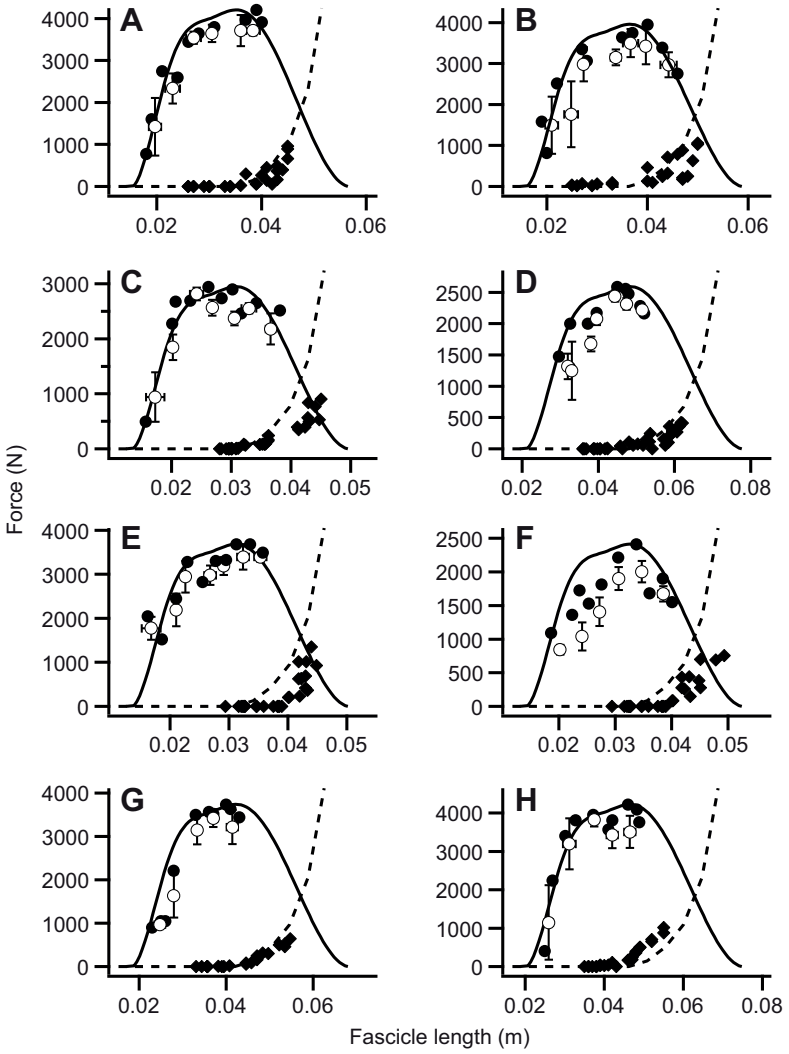

Fig. 3. Active and passive F–L relationship for the right SOL muscle of eight participants (A–H). The filled circles represent experimental data of peak active fascicle force across the range of fascicle lengths taken from repeated MVCs across the ankle range of motion. The open circles represent the means ± s.d. of repeat MVCs grouped according to fascicle length. Mean data were calculated by categorizing MVCs into groups (between 6 and 7) that were divided equally across the fascicle length range so that each length group spanned less than 10% of the optimal fascicle length (L_0). The filled diamonds are experimental data of passive fascicle force. The continuous black curve represents the theoretical whole-muscle active F–L curve and the dashed line represents the theoretical passive fascicle F–L curve [theoretical curves taken from OpenSim; https://simtk.org/home/opensim (Delp et al., 2007)].

Active force–length relationship

All participants exhibited a plateau in the maximum voluntary SOL isometric force production (Fig. 3). Four of the eight participants exhibited the start of the descending limb of the F–L relationship (Figs 3, 4). The estimated L_0 and the peak isometric force from the eight participants were 0.0377±0.0069 m and 3469.4±720.0 N, respectively. Despite some variability, the experimental data approximates the theoretical whole muscle force–length curve with a mean percentage difference between the experimental and theoretical normalized active forces of 10.5±3.0% across all muscle lengths and all participants (Fig. 4). For comparison, we also fitted the experimental data using a standard sarcomere F–L curve using human myofilament lengths (Walker and Schrodt, 1974) and a sliding filament model [(Gordon et al., 1966; Gollapudi and Lin, 2009) L_0 is defined as the mid-point of the plateau]. The fits using either the whole muscle or sarcomere F–L relationship were similar (r^2 of 0.748 and 0.763, respectively) and not statistically different, and the use of a whole muscle *vs* sarcomere curve did not change the findings or conclusions of the study.

Muscle length changes and normalized length operating range during walking and running

Spatiotemporal gait information from walking and running are summarized in Table 1. During the time when the muscle was active, the mean data from all participants during walking is characterized by a moderate stretch–shorten cycle of the SOL primarily across the shallow ascending limb of its F–L curve (Fig. 5A). The start of muscle lengthening and EMG activity is concomitant with the start of ankle dorsiflexion in early stance. The normalized muscle length at start of activation was 0.84±0.15 L_0. By approximately 30–40% of the gait cycle, the muscle lengthened to a maximum of 0.94±0.16 L_0. The increase in mean normalized muscle length during the first half of stance was 0.094±0.088 ($P<0.01$; one-sample t-test). During mid-stance the mean length data exhibited an isometric phase until just prior to the start of plantar flexion. Peak SOL EMG occurred slightly before the start of plantar flexion at a muscle length of 0.88±0.19 L_0. During plantar flexion the muscle shortens as it deactivates, down to 0.74±0.18 L_0 at toe-off, and continues to shorten passively after toe-off to a muscle length of 0.68±0.17 L_0. During the mid-swing phase the SOL lengthens passively to 0.99±0.15 L_0. During the later part of the swing phase and early stance the muscle remains passive and its length change mirrors that of the ankle joint excursion (Fig. 5A).

Because the ultrasound video degraded in one participant during running, mean data for running is derived from seven individuals. In contrast to walking, the mean SOL length shortens throughout the majority of the time the muscle is active (heel-strike to toe-off;

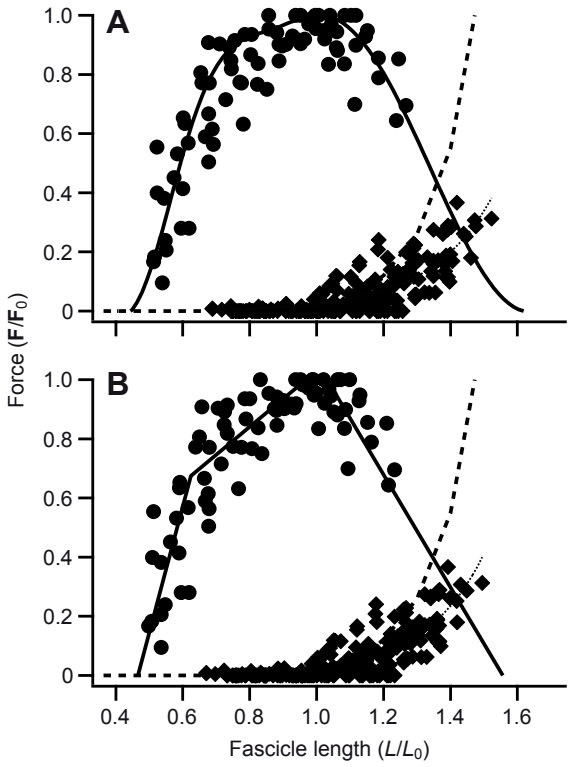

Fig. 4. Pooled normalized active and passive F–L relationship. Data are from the right SOL from eight participants. Data description as per Fig. 3, normalized to individual peak force ($\mathbf{F}_0$) and L_0. (A) Data fitted using a whole-muscle F–L relationship [theoretical curves taken from OpenSim (Delp et al., 2007); r^2=0.748] and (B) using a theoretical sarcomere F–L relationship based on human filament lengths [(Gordon et al., 1966; Walker and Schrodt, 1974; Gollapudi and Lin, 2009); r^2=0.763]. The thin dotted line represents the experimental passive F–L data fitted using Eqn 1.

Fig. 5B). Muscle shortening occurs mainly across the ascending limbs of the muscle's F–L curve. Active muscle shortening started at heel-strike at a normalized length of 0.97±0.10 L_0 and was significantly longer than the length at the onset of muscle activity during walking (P<0.05). During the mid-stance of running, the mean SOL length remains close to isometric. The peak in the SOL EMG signal occurred towards the end of this near-isometric phase at a muscle length of 0.88±0.18 L_0. After toe-off in running, the muscle is inactive and predominantly lengthens during ankle dorsiflexion through the early- and mid-swing phase. At the end of the swing phase the ankle does not change angle and the mean SOL length remains isometric (Fig. 5B).

The total muscle length change increased moderately, although statistically significantly (P<0.05) between walking (12.1±3.5 mm) and running (14.1±3.3 mm). Normalized total muscle length changes likewise increased (P<0.05) between walking (31.7±6.0%) and running (39.0±9.9%), as did the normalized muscle length change during the time the muscle is active (walking, 24.0±3.9%; running, 33.5±7.3%; P<0.05). Despite greater normalized fascicle length changes, the region of the F–L curve occupied by the muscle was similar between the two gaits and not statistically different (Table 2). The normalized muscle length at peak EMG was likewise not statistically different between walking and running. However, we observed in all but two individuals that if the muscle length was below L_0 at peak EMG during walking it increased to a length closer to L_0 at peak EMG in running, and if the muscle length was above L_0 at peak EMG in walking it shortened to a length closer to L_0 at peak EMG in running. The absolute difference between the normalized length at peak EMG and L_0 was 19.1±12.3% for walking and 14.9±12.5% for running. The absolute and normalized muscle length changes during walking and running are summarized in Table 2.

In all but one individual, the SOL occupied mainly the ascending limbs of the F–L curve when active during both walking and running. Nevertheless, the specific region of the F–L curve occupied by the SOL exhibited a moderate degree of variability between participants (shaded region, Fig. 5). This is due, in part, to a single participant whose SOL operated to a large extent on the plateau and descending limb of its F–L curve. Although this length is considerably longer than the other participants, it resides in a physiologically plausible range (Arnold and Delp, 2011) and thus we have retained it in our analysis. As a result, the variability in the reported normalized muscle lengths during gait is greater than if the absolute muscle length is expressed as a percentage of its length at heel strike (mean coefficient of variation of 18.7 *vs* 9.7%, respectively). Muscle lengths were consistent across strides in all individuals; the mean coefficient of variation between five strides across all participants was 7% in walking and running, similar to that reported by Cronin et al. (Cronin et al., 2009).

Correlation between SOL length changes and subject-specific L_0 during walking and running

The absolute length change (mm) of the SOL during walking correlated with subject-specific L_0 so that muscles with longer optimal lengths underwent greater length changes (r=0.84; P<0.01). When normalized to L_0, we observed a negative correlation between the minimal normalized muscle length and L_0 (r=–0.71; P<0.05), indicating that longer muscles operate at shorter normalized lengths. The overall normalized muscle length changes among subjects was, however, independent of L_0 during walking (r=0.37, P=0.365). There were no statistically significant correlations between any length change parameters of the SOL and the L_0 of subjects during running. We also found that the subjects' absolute (mm) muscle length changes were independent of both the Achilles moment arm and the ankle joint angular excursion during walking and running.

Table 1. Spatio-temporal gait parameters

	Speed (treadmill) (m s^{-1})	Speed (overground) (m s^{-1})	Stride time (s)	Stance time (s)	Swing time (s)	Stride frequency (Hz)	Stride length (m)
Walk	1.14±0.16 (1.05–1.40)	1.20±0.31 (1.14–1.59)	1.15±0.06	0.71±0.05	0.44±0.04	0.87±0.05	1.31±0.17
Run	3.0	3.0	0.72±0.04	0.25±0.02	0.47±0.06	1.39±0.07	2.17±0.12

Data are means ± s.d. Walking speed data are for preferred treadmill and overground speeds (range in parentheses). The remaining walking data are from preferred treadmill speeds.

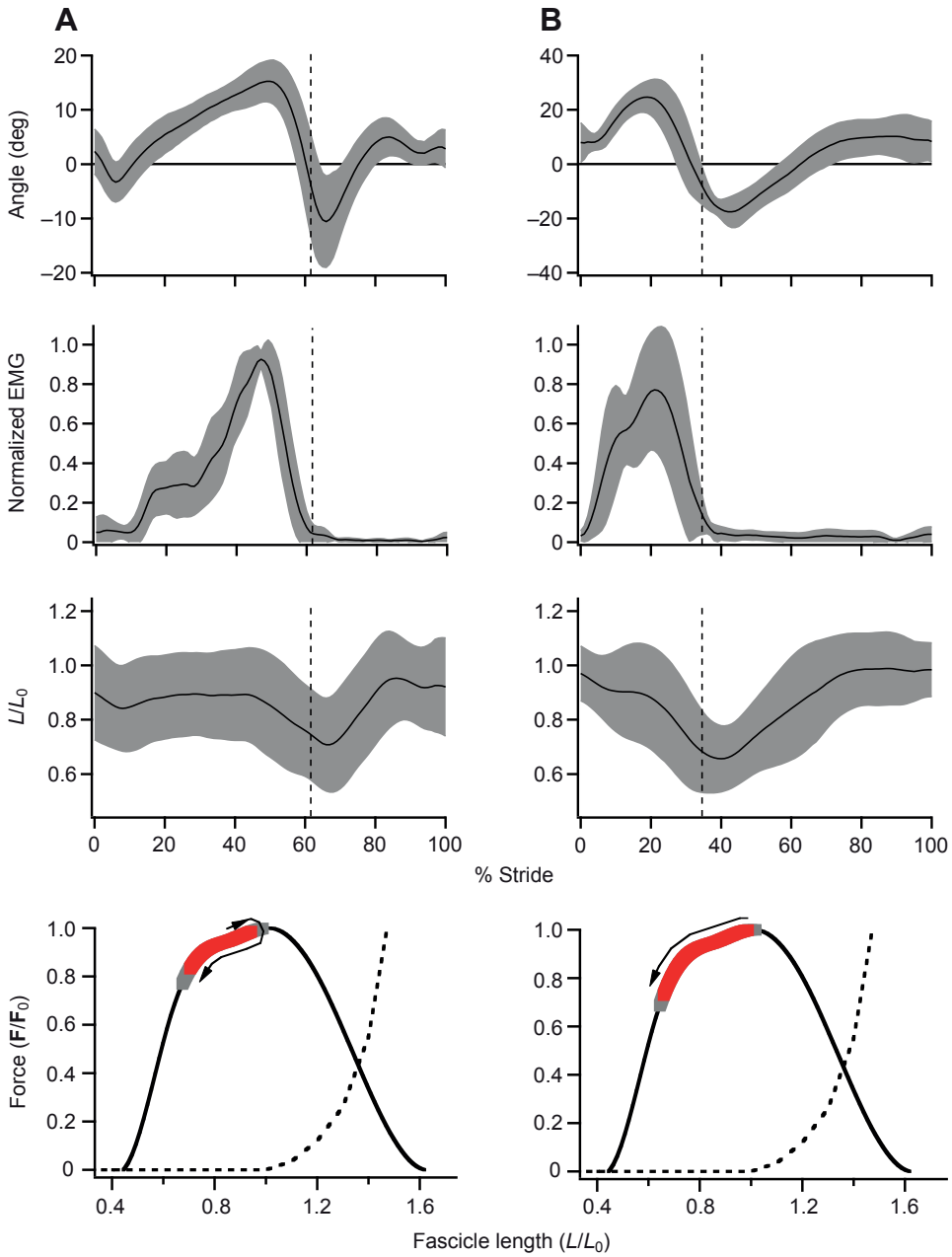

Fig. 5. SOL muscle and joint mechanics during gait. Mean joint angle (panel 1), EMG linear envelope (panel 2), normalized muscle length (L/L_0; panel 3) as a percentage of gait cycle (heel-strike to heel-strike), and the region on the F–L curve occupied by the muscle (panel 4). In panels 1–3, the shaded region represents the s.d. of the mean, and the vertical dotted line represents toe-off. In panel 4, the red and grey lines represent active and inactive muscle lengths across the stride, respectively. The arrow represents the direction of muscle length change from the start to end of muscle activation. (A) Walking at the subjects' preferred treadmill speed. (B) Running at 3 m s^{-1}.

DISCUSSION

SOL strain pattern and normalized length operating range

This study used a novel framework based on a suite of mechanical and musculoskeletal data to experimentally assess the region on the F–L curve occupied by the SOL during gait in humans. We did so using, for the first time, subject-specific assessments of optimal fascicle lengths and dynamic length changes. Our data indicate that the SOL functions primarily across the shallow ascending limb of the F–L relationship in a stretch–shorten cycle during walking in the majority of individuals tested. These data provide among the most direct evidence in humans corroborating the theory that muscles occupy the region of the F–L curve that is matched to its functional requirements (Herzog et al., 1992; Rassier et al., 1999) (although see discussion on running below). Due to the stretch–shorten cycle, the increase and decrease in SOL muscle force required during stance is accompanied by a concomitant increase

Table 2. Summary of soleus muscle fascicle length changes during walking and running

	Total length change (m)	Total length change (L/L_0)	Max. active length L/L_0	Min. active length L/L_0	Active length change (L/L_0)	Length start activation L/L_0	Length end activation L/L_0	L/L_0 at peak EMG
Walk	**0.0121±0.0035**	**0.317±0.058**	0.938±0.165	0.698±0.158	**0.240± 0.039**	**0.845±0.154**	0.736±0.180	0.877±0.188
Run	**0.0141±0.0033**	**0.390±0.099**	0.989±0.110	0.653±0.114	**0.335± 0.072**	**0.968±0.103**	0.669±0.114	0.879±0.180

Data are means ± s.d. L_0 is the subject-specific optimal fascicle length. Values in bold designate a significant difference between walking and running (P<0.05).

and decrease in the capacity for generating force based on its F–L relationship. Interestingly, modulation of force during walking is thus achieved, in part, by the F–L properties of the muscle itself (possibly simplifying neural control). Our finding also supports the theory that muscles occupy the region of the F–L curve where they may be better able to resist lengthening perturbations and injury due to stretch (Julian and Morgan, 1979; Morgan, 1990), avoiding the more unstable descending limb of the F–L curve. A drawback to operating on the ascending limb of the F–L curve is, of course, suboptimal force capacity. However, considering that walking is achieved by submaximal force production, this does not greatly restrict function. It is also worth highlighting that despite operating on the ascending limb, the normalized muscle length of 0.88 L_0 when peak EMG is recorded indicates that the SOL is not greatly restricted in its length-dependent force-generating capacity (~95%) when the greatest muscle activation and force is probably required (electromechanical delay is not expected to greatly affect this conclusion given the small changes in muscle length spanning the peak in EMG).

Although previous experimental data for normalized SOL lengths during walking are (to the best of our knowledge) lacking for human gait, the measured changes in SOL normalized lengths corroborates a recent optimization-based computer simulation (Arnold and Delp, 2011), which predicted a similar pattern across both the stance and swing phases of walking. When these authors used a compliant tendon in their model they predict similar, albeit somewhat longer, normalized muscle lengths that function in a stretch–shorten cycle primarily over the ascending limb and plateau region, and exhibit an isometric phase in mid-stance. Interestingly, the individual in our analysis with the longest normalized muscle lengths exhibited muscle lengthening through dorsiflexion across the plateau region and on to the descending limb of the F–L curve, similar to that predicted by Arnold and Delp (Arnold and Delp, 2011) when using a stiff tendon in their model (their standard model).

Despite requiring different forces (Neptune and Sasaki, 2005), the SOL muscle operates over a similar region on its F–L curve during walking and running, providing among the first experimental evidence in humans of muscle operating ranges being conserved across different gait mechanics. The overall length operating range is thus not modulated to accommodate an increase in the muscle force required in the human SOL during running. Interestingly, a similar region of the F–L curve is used even though the muscle has a fundamentally different length pattern, whereby the muscle undergoes near continuous shortening during the stance-phase opposed to the stretch–shorten cycle observed in walking (Fig. 5B). This pattern of length change is similar to that measured during running in the MG muscle (Lichtwark et al., 2007) and thus may be a general characteristic of the triceps surae.

A consequence of the length pattern is that the region of the F–L curve used during running does not match the functional requirement of the muscle in the same sense as in walking. When running, an increase in force required during stance is accompanied by a decrease in the length-dependent force-generating capacity of the muscle as it shortens. It remains possible that operating on the ascending limb of the F–L curve during running is a strategy adopted to prevent unstable lengthening perturbations that can occur when operating on the descending limb of the F–L curve, and may contribute to tension regulation in the SOL (Pinniger et al., 2000). Thus, resistance to muscle perturbation may dictate the length operating range during running more so than matching the muscle's length pattern to its *in vivo* force requirement (as would be the case if the muscle shortened on the descending limb of the F–L curve). Considering that the ankle joint undergoes rapid dorsiflexion during the first part of stance (as the Achilles tendon stretches), unexpected ankle perturbations may indeed lead to significant SOL lengthening. The possibility of rapid SOL lengthening during walking has recently been shown to occur experimentally under induced perturbations (Cronin et al., 2009). Alternatively, conserving function to the ascending limb may also be linked with optimizing the release of stored elastic energy in the Achilles tendon. Deactivating the SOL during shortening on the ascending limb increases the rate of force decay, and thus the return of stored elastic energy in the tendon (tendon power generation). In contrast, if the SOL shortens on the descending limb, the force capacity would increase during deactivation and limit the rate of force decay and tendon power.

As is the case in walking, the length operating range during running does not greatly limit its force-generating capacity at peak EMG, which probably approximates the time when peak activation and muscle force is required. This is accomplished by the muscle starting to shorten at a considerably longer muscle length during running compared with the length at the start of muscle activity in walking (0.97 *vs* 0.85 L_0), allowing it to remain close to L_0 at mid-stance when peak EMG is recorded (0.88 L_0). The operating length appears to be controlled so that during both walking and running the muscle achieves an operating range across the ascending limb whilst conserving a near-optimal (~95%) length-dependent force-generating capacity around the time the highest forces are required.

It is worth noting that, whereas the mean normalized muscle length at peak EMG across all participants is not different between walking and running, this does not reflect the small shift to muscle lengths closer to L_0 at peak EMG during running in five of the subjects tested. This finding suggests that a strategy may exist to increase the force-generating capacity during the time peak force is required in some individuals. In this regard we cannot rule out entirely the premise that muscle operating lengths are modulated to accommodate an increase in force requirement between walking and running. However, given that the shift towards the plateau region is small (resulting in a predicted increase in force capacity of less than 5%) and since the overall normalized length range is not different between gaits, any such modulation is minimal. Furthermore, the increase in length-dependent force capacity in running may be offset by the decrement in force-producing capacity as a result of force–velocity effects. Whether a more distinct modulation in muscle lengths occurs in tasks requiring maximal forces, such as those during sprinting or maximal vertical jumps, remains possible. It should also be stressed that our analyses are restricted to a relatively small portion of the muscle and therefore the average region on the F–L curve occupied by all muscle fibres may be different than that reported here. This can occur if there are regional differences in muscle fascicle strain [although it has been found that, at least for the human MG, these differences are relatively small during walking and running (Lichtwark et al., 2007)] or between-fibre sarcomere length heterogeneity.

Inter-individual variation in SOL length changes during walking and running and correlation with subject-specific L_0

We found that the region of the F–L curve occupied by the muscle was similar across most participants. However, inter-individual variation in the SOL operating lengths did exist, with a ~40% difference in the longest and shortest normalized operating length observed among participants. This is similar to the 36% difference observed between the shortest and longest optimal fascicle lengths (L_0) among the participants (0.031–0.048 m). One might logically expect that the participants with the shortest L_0 will exhibit the

longest normalized operating lengths and thus operate further to the right on their F–L curve, and to exhibit the greatest overall change in normalized fascicle lengths. This was supported only by a negative correlation between the minimal normalized muscle length and L_0 during walking. In contrast, however, the total change in normalized fascicle lengths and the overall region occupied on the F–L curve over the stride and during the time the muscle was active did not show statistically significant correlations with L_0 in walking or running. Interestingly, the lack of correlation between the operating region on the F–L curve and L_0 during walking results because muscles with shorter L_0 undergo smaller absolute length changes (mm) so that the normalized length range remains constant across subjects. This finding provides among the first experimental evidence in humans of muscle lengths being governed in a manner to conserve their operating range on the F–L curve. Exactly what the underlying musculoskeletal mechanisms are that allow for the normalized muscle operating range to be independent of L_0 in walking and running nevertheless remains unclear. The ratio of moment arm to fibre length has been suggested to be one such mechanism (Lieber and Ward, 2011). A greater moment arm to fibre length ratio will result in greater changes in fascicle length for a given joint excursion. A proportional increase in moment arm with increasing L_0 across subjects would thus be expected. However, we found no correlation between the Achilles moment arm and L_0. We also found no correlation between the absolute SOL length change (mm) and ankle angular excursion among participants during walking and running. Other factors such as Achilles tendon stiffness, which will alter muscle lengths, or muscle activation conditions (Lichtwark and Wilson, 2005) may function to regulate the operating region of the muscle on the F–L curve during gait.

Subject-specific force–length curves

As well as informing where the SOL functions on its F–L curve during gait, the present study provides novel information on the active and passive SOL F–L relationships themselves. Compared with previous work, the mean SOL L_0 and estimated peak force measured in the eight participants were only marginally different from that reported by Maganaris (Maganaris, 2001), who used a similar experimental protocol. Our experimental values are also in good agreement with the estimated mean L_0 from anatomical measurements [(Ward et al., 2009) L_0=0.044 m]. In addition, we have shown that experimental normalized maximal isometric F–L data from the SOL approximate the theoretical whole muscle and sarcomere (based on human filament lengths) F–L curves (Fig. 4). The match between experimental F–L data of the human SOL and the theoretical F–L curve is not substantially different from that recently reported for rabbit muscle using *in situ* muscle preparations (Winters et al., 2011). The region of the F–L curve occupied by the SOL also closely matches the prediction using a recent musculoskeletal model (Arnold et al., 2010) of the muscle undergoing maximal isometric contractions across the same range of ankle angles as those measured in this study. Together, these findings suggest that F–L profile of the region of the muscle imaged has been accurately represented.

Our estimates of the passive F–L curves of the SOL fascicles were consistently less steep than the theoretical model (Fig. 4) and compared to those from other mammalian species (Azizi and Roberts, 2010), despite the peak passive muscle forces and stiffness being commensurate with those reported for the human gastrocnemius muscle (Hoang et al., 2007; Gao et al., 2009) (taking into account muscle cross-sectional area). Our results show that the length at which passive SOL forces begin to develop correspond closely to the predicted L_0, corroborating both standard models (Zajac, 1989) and previous experimental data (Azizi and Roberts, 2010; Winters et al., 2011), and provides further confidence in our estimates of subject-specific F–L data. The close association between the length at the initiation of passive force and L_0 may provide a convenient and less experimentally intensive approach to establishing subject-specific muscle properties for both experimental and computer simulation studies of human muscle function.

Confounding factors influencing muscle length-dependent force capacity

While the goal of the present study was to understand what region of the maximal isometric F–L curve the SOL operates over during walking and running, it does not assess other factors that may influence length-dependent force-generating capacity. In submaximally activated skinned fibres and intact muscle preparations, peak isometric forces occur at longer lengths compared with L_0 measured during maximal activation (Rack and Westbury, 1969; Rassier et al., 1999). Because the SOL is submaximally activated during walking and running, the actual *in vivo* length-dependent force-generating capacity may be somewhat lower than those reported here. However, given that the altered shape of the F–L curve in submaximal contraction is related to the rate of action potential impulses, and since larger muscles including the SOL have been reported to have less scope for rate coding (Bellemare et al., 1983; De Luca, 1985), differences may be small. It is also well accepted that the isometric length-dependent force-generating capacity of a muscle is influenced by prior changes in muscle length under the same activation period [muscle history dependence (Rassier and Herzog, 2004; Pinniger and Cresswell, 2007)]. Given the opposite direction of muscle length changes in early stance of walking and running it is possible that history-dependent effects lead to a difference in force capacity during mid-stance in these gaits. However, any interpretations on activation- and history-dependent effects should be considered with caution, given that neither is well understood during voluntary contractions in dynamic movement tasks such as walking and running.

CONCLUSIONS

The results of this study indicate that the SOL operating region on the F–L curve is highly conserved across walking and running gaits, despite gait-dependent differences in muscle–tendon dynamics. Our finding that the muscle functions predominantly across the ascending limbs of its F–L curve provides new experimental support for the theory that skeletal muscles function in a manner that optimizes stable force production compared with optimal force output during walking and running. Whether this is true across a diverse range of muscles and locomotor tasks, however, requires further analysis. A common SOL operating range is observed, despite relatively large differences in L_0 among subjects, and is achieved through a positive correlation between the L_0 of subjects and the absolute muscle length change during gait. Finally, although the SOL seldom functions at the plateau of its F–L curve during walking and running, its length-dependent force capacity (based on the muscle's maximal isometric F–L curve) nevertheless remains high during the time peak forces are required.

APPENDIX

Influence of ultrasound probe positioning and movement on fascicle length measurements

One of the key requirements of this study was a consistent position of the ultrasound probe across experimental sessions. In order to

ensure that the subjects' probe location was the same between dynamometer and treadmill trials, a marker set was placed on the probe and on the malleoli and femoral condyles, allowing the location of the probe relative to the leg to be assessed. In addition, the rotation of the probe about the long axis of the leg was estimated using a hand-held goniometer and the depth of the muscle was measured at the external and internal aponeuroses. In order to rapidly estimate the probe location, an outline of the probe placement on the calf was also made with an insoluble ink pen.

The repeatability of probe placement was assessed by calculating the coefficient of variation in passive muscle fascicle length at a neutral ankle angle (0 deg) between three separate probe placements. The small coefficient of variation (2.4±0.7%) indicates that the probe was reliably positioned throughout the experiment. Probe movement during gait may also have affected muscle length measurements. From 3D motion capture data of the probe, we computed approximately 5 deg of motion between the probe and tibia during running, both about the long axis and the adduction/abduction axis of the tibia (e.g. long axis and medio/lateral rotation of the probe). In order to assess the potential error in length measurements due to probe movement we simultaneously measured muscle lengths and 3D probe and tibia position while systematically moving the probe through a range motion by hand. We estimated ~4% error in muscle lengths over a similar range of motion observed during running. However, even this small error may be an overestimate since measured probe movement during gait is due, in part, to movement of the muscle mass itself rather than the probe relative to the muscle. Proximal/distal and anterior/posterior movement (the latter induced by compressing the calf musculature) had a negligible effect on muscle length measurements. Although the effect of probe position and movement has a minimal effect on the measurement of the normalized length operating range for the fascicles imaged, because our analyses are restricted to a relatively small portion of the muscle we can nevertheless not rule out that the average region on the F–L curve occupied by all muscle fibres may be different than that reported here.

Assessment of maximal torque and muscle force

Inhibition of voluntary muscle activation is typically assessed using a twitch-interpolation protocol, whereby muscle stimulation is used to evoke a superimposed twitch torque during a voluntary contraction. The experimental setup prevented us from conveniently conducting simultaneous EMG, ultrasonography and electrical stimulation recordings. We performed twitch interpolation measurements on subjects in a separate testing session in order to assess their potential to fully activate their ankle plantar flexor muscle group under the same conditions as those of the F–L experiment. Three supramaximal doublets (pulse width 100 µs, inter-twitch interval 10 ms) were administered percutaneously using surface electrodes (Carbo Stim, Medi-Stim, Wabasha, MN, USA) positioned over the proximal (anode; 4.4×9.5 cm) and distal (cathode; 4.4×4.4 cm) calf musculature. Two doublets separated by 1 s were administered after the MVC torque had reached a plateau. The third doublet was administered after relaxation. The doublet amplitude was determined by increasing the twitch voltage until twitch torque ceased to increase with a further 10 V increment (S88K, Grass Technologies, West Warwick, RI, USA). The per cent activation (per cent maximal force) during the voluntary contraction was estimated as: voluntary activation = [1 – (superimposed moment/potentiated resting moment)]×100. In order to assess whether voluntary activation was affected by joint posture we performed 3–4 twitch interpolation measurements (separated by 2 min) at a maximal dorsiflexion angle, a neutral angle (0 deg) and a plantar flexed angle (–15 deg).

The twitch interpolation experiment confirmed that participants were capable of either fully activating their plantar flexor muscle group (100% activation) or near-maximal activation (>95%) at all three angles (Fig. A1). We also observed near-constant EMG amplitude of the MG, LG and SOL during the MVCs. This analysis indicates that the MVC protocol adopted in our F–L analysis closely reflects the maximal activation of the SOL. Even had there been a moderate gradation of inactivation across the joint range of motion, the effect on L_0 would probably be small; assuming a linear gradation from 10% inactivity at the shortest lengths to 0% inactivity at the

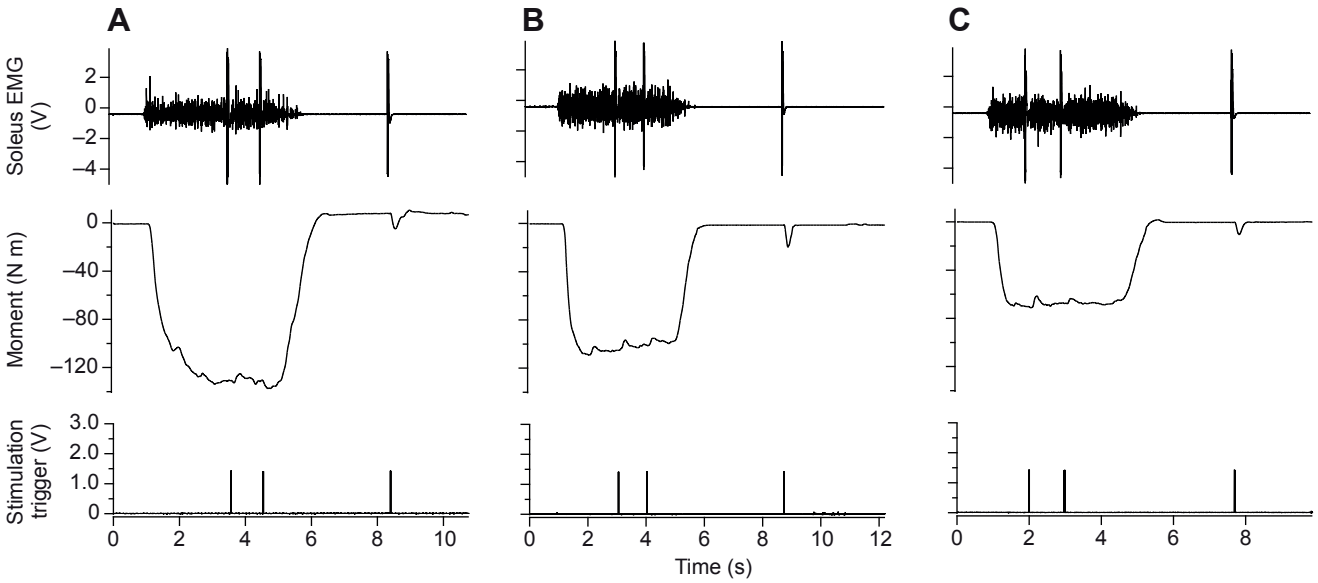

Fig. A1. Representative twitch interpolation results for MVCs at (A) maximal dorsiflexion, (B) neutral angle (0 deg) and (C) –15 deg plantar flexion.

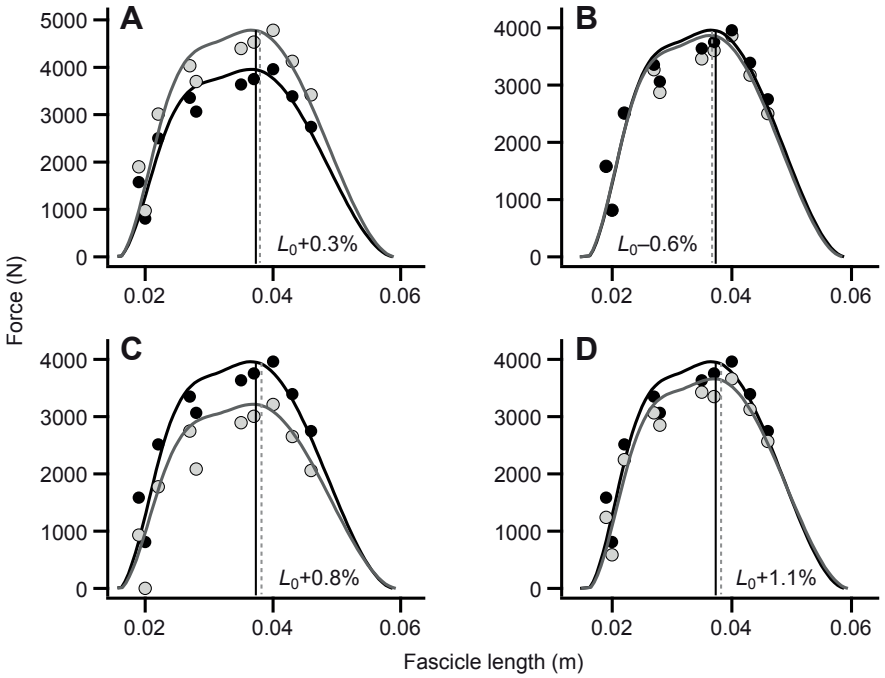

Fig. A2. A sensitivity analysis of the estimation of optimal fascicle length (L_0) using representative subject data. The effect of (A) an increase in the angle-specific Achilles moment arm of ×1.2 during MVC (black) *vs* maintaining a constant moment arm between rest and MVC (grey); (B) reduction in passive SOL force between rest and MVC (black) *vs* constant angle-specific passive SOL force (grey); (C) a negligible synergist muscle contribution to the measured MVC moment (black) *vs* including a hypothetical maximal synergist muscle contribution (grey); and (D) a prediction of antagonist (co-contraction) force from the TA muscle (black) *vs* no co-contraction contribution to the measured MVC moment (grey). The data points represent the estimated maximal isometric SOL force across muscle lengths (black circles, forces used in present study; grey circles, effected forces) and the thick black and grey curve represents the corresponding theoretical F–L curves (L_0 determined using a least-squares non-linear optimization routine). The vertical continuous and dotted lines represent the L_0 used in the present study and the effected L_0, respectively (including the percent difference in the estimate of L_0).

longest lengths, and *vice versa*, resulted in an estimated L_0 that was 0.8% shorter and 1.1% longer, respectively.

Errors in dynamometer-based estimates of peak ankle moments arise due to small, unavoidable misalignments between the dynamometer and ankle axes of rotation during plantar flexion (Arampatzis et al., 2007). Our experimental setup limited these movements to 5.7±2.4 mm along the foot's long axis. Following the study of Arampatzis et al. (Arampatzis et al., 2007) (assuming a centre of pressure aligned with the first metatarsal) we estimated that this movement resulted in a maximum of 4–5% overestimate of ankle joint moment. These errors were consistent and not significantly different across plantar flexed and dorsiflexed positions, and therefore, while slightly overestimating muscle force, would not have affected the shape of the normalized SOL F–L curve.

To take into account the increase in the Achilles moment arm that has been reported between rest and MVC, we multiplied the moment arm at MVC by a factor of 1.2 (Maganaris, 2004). The application of this correction factor lowered the calculated maximal forces but a sensitivity analysis indicates a negligible (<1%) effect on the shape of the F–L curve and on the estimate of subject-specific L_0 (Fig. A2A).

Influence of passive SOL force on estimates of L_0

Our estimate of the reduction in passive force during MVCs (due to muscle shortening prior to its isometric phase) assumed that all of the passive muscle moment at the ankle was attributed to the SOL. This assumption is supported in our participants both from constant MVC force at maximal dorsiflexion across knee angles of 130–110 deg as well as from muscle force predictions at matched knee and ankle angles using a recent musculoskeletal model [OpenSim (Arnold et al., 2010)]. Passive forces may also occur in other joint structures (e.g. bone, ligaments, skin), although the Achilles tendon has been found to be the primary structure limiting ankle joint dorsiflexion, and thus is probably the major contributor to passive force within a physiological joint range of motion (Costa et al., 2006). A sensitivity analysis found that any errors in predicting reductions in passive muscle force during MVC will have a small effect on the shape of the F–L curve and the assessment of subject-specific L_0; when the reduction in passive forces is ignored, the estimate of L_0 is altered by less than 1% (Fig. A2B).

Influence of synergist and antagonist muscle force on estimates of L_0

Our approach assumed that the SOL was the only muscle responsible for active muscle force and joint moment production when the knee was flexed past 120 deg. The failure to increase ankle plantar flexion moments at maximal dorsiflexion with increasing knee angles (130–110 deg) in our participants supports this assumption. Nevertheless, the possibility that small contributions to the measured joint moments are attributed to synergist muscles cannot be unequivocally ruled out. In order to assess the possible errors associated with synergist muscle force production, we used the OpenSim musculoskeletal model of Arnold et al. (Arnold et al., 2010) to predict the plantar flexion moment contribution from the MG and LG, tibialis posterior, peroneus longus and brevis, flexor hallucis longus and flexor digitorum longus, assuming maximal activation ('worst-case' scenario). Although this analysis predicted a reduction in SOL force, we found that contributions from synergist muscles affected the prediction of L_0 by approximately 1% (Fig. A2C).

The contribution of antagonist muscle force in the TA muscle was predicted and applied to our estimates of SOL force production. The activation level of the TA in each plantar flexion trial was taken as the ratio of the r.m.s. of the TA EMG signal in the plantar flexion MVC and the peak value from the baseline dorsiflexion MVCs. The TA activation ratio and ankle joint angle data for each individual plantar flexion trial were input into a subject-specific scaled OpenSim model (Arnold et al., 2010) to predict the TA muscle moment. The predicted TA moment from OpenSim was subsequently scaled using the ratio of the maximal experimental dorsiflexion moment at 0 deg ankle angle and that predicted by the model under maximal activation. In order to assess how sensitive the estimate of L_0 is to possible errors in our prediction of antagonist force production we calculated F–L

data assuming zero co-contraction ('worst-case' scenario). This analysis found that the estimate of L_0 increased by approximately 1% (Fig. A2D).

LIST OF SYMBOLS AND ABBREVIATIONS

EMG	electromyography
F–L	force–length
$\mathbf{F}_{SOLa}$	active soleus fascicle force
$\mathbf{F}_{SOLp}$	passive soleus fascicle force
$\mathbf{F}_{TENDp}$	passive force in the Achilles tendon
L_0	optimal fascicle length
L_s	fascicle length at which passive forces begin
LG	lateral gastrocnemius
$\mathbf{M}_{foot}$	ankle moment generated by the weight of the foot
$\mathbf{M}_{peak}$	peak net ankle joint moment
$\mathbf{M}_{rig}$	dynamometer moment generated by foot rig
$\mathbf{M}_{SOLa}$	soleus active ankle moment
$\mathbf{M}_{SOLp}$	soleus passive ankle moment
$\mathbf{M}_{TA}$	dorsiflexion moment generated by the tibialis anterior
$\mathbf{M}_{tot}$	total moment measured at the dynamometer
MG	medial gastrocnemius
MVC	maximal voluntary isometric contraction
$\mathbf{r}_{SOL}$	soleus ankle moment arm
SOL	soleus
TA	tibialis anterior
TTL	transistor–transistor logic
θ_{pen}	soleus pennation angle

ACKNOWLEDGEMENTS

The authors would like to thank Fausto Panizzolo for helping with aspects of probe placement validation, Edith Arnold for sharing the musculoskeletal model, and The University of Western Australia School of Sport Science, Exercise and Health 'Biomechanics Journal Club' for helpful discussions regarding this study.

FUNDING

This work was supported by a Grant-in-Aid (G 09P 4469) from the National Heart Foundation of Australia and a University of Western Australia Research Development Award to J.R.

REFERENCES

Abramoff, M. D., Magelhaes, P. J. and Ram, S. J. (2004). Image processing with ImageJ. *Biophotonics Int.* **11**, 36-42.
An, K. N., Takahashi, K., Harrigan, T. P. and Chao, E. Y. (1984). Determination of muscle orientations and moment arms. *J. Biomech. Eng.* **106**, 280-282.
Arampatzis, A., De Monte, G. and Morey-Klapsing, G. (2007). Effect of contraction form and contraction velocity on the differences between resultant and measured ankle joint moments. *J. Biomech.* **40**, 1622-1628.
Arnold, E. M. and Delp, S. L. (2011). Fibre operating lengths of human lower limb muscles during walking. *Philos. Trans. R. Soc. B* **366**, 1530-1539.
Arnold, E. M., Ward, S. R., Lieber, R. L. and Delp, S. L. (2010). A model of the lower limb for analysis of human movement. *Ann. Biomed. Eng.* **38**, 269-279.
Azizi, E. and Roberts, T. J. (2010). Muscle performance during frog jumping: influence of elasticity on muscle operating lengths. *Proc. R. Soc. Lond. B* **277**, 1523-1530.
Behm, D. G., St-Pierre, D. M. and Perez, D. (1996). Muscle inactivation: assessment of interpolated twitch technique. *J. Appl. Physiol.* **81**, 2267-2273.
Bellemare, F., Woods, J. J., Johansson, R. and Bigland-Ritchie, B. (1983). Motor-unit discharge rates in maximal voluntary contractions of three human muscles. *J. Neurophysiol.* **50**, 1380-1392.
Besier, T. F., Sturnieks, D. L., Alderson, J. A. and Lloyd, D. G. (2003). Repeatability of gait data using a functional hip joint centre and a mean helical knee axis. *J. Biomech.* **36**, 1159-1168.
Burkholder, T. J. and Lieber, R. L. (2001). Sarcomere length operating range of vertebrate muscles during movement. *J. Exp. Biol.* **204**, 1529-1536.
Costa, M. L., Logan, K., Heylings, D., Donell, S. T. and Tucker, K. (2006). The effect of Achilles tendon lengthening on ankle dorsiflexion: a cadaver study. *Foot Ankle Int.* **27**, 414-417.
Cronin, N. J., Ishikawa, M., Grey, M. J., af Klint, R., Komi, P. V., Avela, J., Sinkjaer, T. and Voigt, M. (2009). Mechanical and neural stretch responses of the human soleus muscle at different walking speeds. *J. Physiol.* **587**, 3375-3382.
Cutts, A. (1989). Sarcomere length changes in muscles of the human thigh during walking. *J. Anat.* **166**, 77-84.
Delp, S. L., Anderson, F. C., Arnold, A. S., Loan, P., Habib, A., John, C. T., Guendelman, E. and Thelen, D. G. (2007). OpenSim: open-source software to create and analyze dynamic simulations of movement. *IEEE Trans. Biomed. Eng.* **54**, 1940-1950.
De Luca, C. J. (1985). Control properties of motor units. *J. Exp. Biol.* **115**, 125-136.
Fukunaga, T., Kawakami, Y., Kubo, K. and Kanehisa, H. (2002). Muscle and tendon interaction during human movements. *Exerc. Sport Sci. Rev.* **30**, 106-110.
Gao, F., Grant, T. H., Roth, E. J. and Zhang, L. Q. (2009). Changes in passive mechanical properties of the gastrocnemius muscle at the muscle fascicle and joint levels in stroke survivors. *Arch. Phys. Med. Rehabil.* **90**, 819-826.
Gollapudi, S. K. and Lin, D. C. (2009). Experimental determination of sarcomere force-length relationship in type-I human skeletal muscle fibers. *J. Biomech.* **42**, 2011-2016.
Gordon, A. M., Huxley, A. F. and Julian, F. J. (1966). The variation in isometric tension with sarcomere length in vertebrate muscle fibres. *J. Physiol.* **184**, 170-192.
Hamner, S. R., Seth, A. and Delp, S. L. (2010). Muscle contributions to propulsion and support during running. *J. Biomech.* **43**, 2709-2716.
Herbert, R. D., Clarke, J., Kwah, L. K., Diong, J., Martin, J., Clarke, E. C., Bilston, L. E. and Gandevia, S. C. (2011). *In vivo* passive mechanical behaviour of muscle fascicles and tendons in human gastrocnemius muscle-tendon units. *J. Physiol.* **589**, 5257-5267.
Herzog, W., Leonard, T. R., Renaud, J. M., Wallace, J., Chaki, G. and Bornemisza, S. (1992). Force-length properties and functional demands of cat gastrocnemius, soleus and plantaris muscles. *J. Biomech.* **25**, 1329-1335.
Hill, A. V. (1953). The mechanics of active muscle. *Proc. R. Soc. Lond. B* **141**, 104-117.
Hoang, P. D., Herbert, R. D., Todd, G., Gorman, R. B. and Gandevia, S. C. (2007). Passive mechanical properties of human gastrocnemius muscle tendon units, muscle fascicles and tendons *in vivo*. *J. Exp. Biol.* **210**, 4159-4168.
Hodgson, J. A., Finni, T., Lai, A. M., Edgerton, V. R. and Sinha, S. (2006). Influence of structure on the tissue dynamics of the human soleus muscle observed in MRI studies during isometric contractions. *J. Morphol.* **267**, 584-601.
Hof, A. L. and van den Berg, J. (1977). Linearity between the weighted sum of the EMGs of the human triceps surae and the total torque. *J. Biomech.* **10**, 529-539.
Julian, F. J. and Morgan, D. L. (1979). Intersarcomere dynamics during fixed-end tetanic contractions of frog muscle fibres. *J. Physiol.* **293**, 365-378.
Kawakami, Y., Amemiya, K., Kanehisa, H., Ikegawa, S. and Fukunaga, T. (2000). Fatigue responses of human triceps surae muscles during repetitive maximal isometric contractions. *J. Appl. Physiol.* **88**, 1969-1975.
Lichtwark, G. A. and Wilson, A. M. (2005). Effects of series elasticity and activation conditions on muscle power output and efficiency. *J. Exp. Biol.* **208**, 2845-2853.
Lichtwark, G. A., Bougoulias, K. and Wilson, A. M. (2007). Muscle fascicle and series elastic element length changes along the length of the human gastrocnemius during walking and running. *J. Biomech.* **40**, 157-164.
Lieber, R. L. and Ward, S. R. (2011). Skeletal muscle design to meet functional demands. *Philos. Trans. R. Soc. B* **366**, 1466-1476.
Lutz, G. J. and Rome, L. C. (1994). Built for jumping: the design of the frog muscular system. *Science* **263**, 370-372.
MacIntosh, B. R. and MacNaughton, M. B. (2005). The length dependence of muscle active force: considerations for parallel elastic properties. *J. Appl. Physiol.* **98**, 1666-1673.
Maganaris, C. N. (2001). Force-length characteristics of *in vivo* human skeletal muscle. *Acta Physiol. Scand.* **172**, 279-285.
Maganaris, C. N. (2004). Imaging-based estimates of moment arm length in intact human muscle-tendons. *Eur. J. Appl. Physiol.* **91**, 130-139.
Manal, K., Cowder, J. D. and Buchanan, T. S. (2010). A hybrid method for computing Achilles tendon moment arm using ultrasound and motion analysis. *J. Appl. Biomech.* **26**, 224-228.
Martin, D. C., Medri, M. K., Chow, R. S., Oxorn, V., Leekam, R. N., Agur, A. M. and McKee, N. H. (2001). Comparing human skeletal muscle architectural parameters of cadavers with *in vivo* ultrasonographic measurements. *J. Anat.* **199**, 429-434.
McGowan, C. P., Kram, R. and Neptune, R. R. (2009). Modulation of leg muscle function in response to altered demand for body support and forward propulsion during walking. *J. Biomech.* **42**, 850-856.
Morgan, D. L. (1990). New insights into the behavior of muscle during active lengthening. *Biophys. J.* **57**, 209-221.
Narici, M. V. and Maganaris, C. N. (2007). Plasticity of the muscle-tendon complex with disuse and aging. *Exerc. Sport Sci. Rev.* **35**, 126-134.
Neptune, R. R. and Sasaki, K. (2005). Ankle plantar flexor force production is an important determinant of the preferred walk-to-run transition speed. *J. Exp. Biol.* **208**, 799-808.
Neptune, R. R., Sasaki, K. and Kautz, S. A. (2008). The effect of walking speed on muscle function and mechanical energetics. *Gait Posture* **28**, 135-143.
Pinniger, G. J. and Cresswell, A. G. (2007). Residual force enhancement after lengthening is present during submaximal plantar flexion and dorsiflexion actions in humans. *J. Appl. Physiol.* **102**, 18-25.
Pinniger, G. J., Steele, J. R., Thorstensson, A. and Cresswell, A. G. (2000). Tension regulation during lengthening and shortening actions of the human soleus muscle. *Eur. J. Appl. Physiol.* **81**, 375-383.
Rack, P. M. and Westbury, D. R. (1969). The effects of length and stimulus rate on tension in the isometric cat soleus muscle. *J. Physiol.* **204**, 443-460.
Ralston, H. J. (1958). Energy-speed relation and optimal speed during level walking. *Int. Z. Angew. Physiol.* **17**, 277-283.
Rassier, D. E. and Herzog, W. (2004). Considerations on the history dependence of muscle contraction. *J. Appl. Physiol.* **96**, 419-427.
Rassier, D. E., MacIntosh, B. R. and Herzog, W. (1999). Length dependence of active force production in skeletal muscle. *J. Appl. Physiol.* **86**, 1445-1457.
Rome, L. C. and Sosnicki, A. A. (1991). Myofilament overlap in swimming carp. II. Sarcomere length changes during swimming. *Am. J. Physiol.* **260**, C289-C296.
Rome, R. (1998). Matching muscle performance to changing demand. In *Principles of Animal Design* (ed. R. W. Ewald, C. R. Taylor and L. Bolis), pp. 103-113. Cambridge, UK: Cambridge University Press.

Rubenson, J., Heliams, D. B., Maloney, S. K., Withers, P. C., Lloyd, D. G. and Fournier, P. A. (2007). Reappraisal of the comparative cost of human locomotion using gait-specific allometric analyses. *J. Exp. Biol.* **210**, 3513-3524.
Sasaki, K. and Neptune, R. R. (2006). Muscle mechanical work and elastic energy utilization during walking and running near the preferred gait transition speed. *Gait Posture* **23**, 383-390.
Walker, S. M. and Schrodt, G. R. (1974). I segment lengths and thin filament periods in skeletal muscle fibers of the Rhesus monkey and the human. *Anat. Rec.* **178**, 63-81.
Ward, S. R., Eng, C. M., Smallwood, L. H. and Lieber, R. L. (2009). Are current measurements of lower extremity muscle architecture accurate? *Clin. Orthop. Relat. Res.* **467**, 1074-1082.
Winter, D. A. (1990). *Biomechanics and Motor Control of Human Movement.* New York, NY: John Wiley and Sons.
Winters, T. M., Takahashi, M., Lieber, R. L. and Ward, S. R. (2011). Whole muscle length-tension relationships are accurately modeled as scaled sarcomeres in rabbit hindlimb muscles. *J. Biomech.* **44**, 109-115.
Wu, G., Siegler, S., Allard, P., Kirtley, C., Leardini, A., Rosenbaum, D., Whittle, M., D'Lima, D. D., Cristofolini, L., Witte, H. et al. (2002). ISB recommendation on definitions of joint coordinate system of various joints for the reporting of human joint motion – part I: ankle, hip, and spine. *J. Biomech.* **35**, 543-548.
Zajac, F. E. (1989). Muscle and tendon: properties, models, scaling and application to biomechanics and motor control. *Crit. Rev. Biomed. Eng.* **17**, 359-411.